J Neurooncol (2007) 85:111–122
DOI 10.1007/s11060-007-9394-3

LAB INVESTIGATION—HUMAN/ANIMAL TISSUE

# *FOXG1* dysregulation is a frequent event in medulloblastoma

**Adekunle M. Adesina · Yummy Nguyen · Vidya Mehta · Hidehiro Takei · Patrick Stangeby · Sonya Crabtree · Murali Chintagumpala · Mary K. Gumerlock**

Received: 12 February 2007 / Accepted: 17 April 2007 / Published online: 24 May 2007


**Abstract** Medulloblastomas represent 20% of malignant brain tumors of childhood. Although, they show multiple, non-random genomic alterations, no common, early genetic event involving all histologic types of medulloblastomas have been described. Nineteen medulloblastomas were analyzed using chromosomal comparative genomic hybridization (cCGH). Nine tumors with the most frequent number of genetic changes were further analyzed using bacterial artificial chromosome array CGH (aCGH). With aCGH, the frequency of gains and losses were higher than with cCGH. Chromosome 2p gains spanning 2p11–2p25 including *N-myc* locus, 2p24.1 were detected in 5/9 (55%) tumors while 14q12 gains were detected in 6/9 (67%) tumors. The 14q12 locus overlapped with the *FOXGI* gene locus. Quantitative real time PCR showed a 2–7-fold copy gain for *FOXG1* in all the nine tumors. Protein expression was demonstrated by immunohistochemistry in all histologic types. The expression of *FOXG1* and *p21cip1* showed an inverse relationship. *FOXG1* copy gain (>2 to 21 folds) was seen in 93% (55/59) of a validating set of tumors and showed a positive correlation with protein expression (Spearman's rank order correlation coefficient = 0.276; $P = 0.038$) representing the first report of *FOXG1* dysregulation in medulloblastoma. Modulation of *FOXG1* expression in DAOY cell line using siRNA showed a modest decrease in proliferation with a 2-fold upregulation of p21cip1. Current reports indicate that *FOXG1* represses *TGF-β* induced expression of *p21cip1* and cytostasis, and forms a transcriptional repressor complex with *Notch* signaling induced *hes1*. Our findings are consistent with a role for *FOXG1* in the inhibition of *TGF-β* induced cytostasis in medulloblastoma.

**Keywords** Array comparative genomic hybridization · *FOXG1* · medulloblastoma · *p21cip1* · Pediatric brain tumors · Primitive neuroectodermal tumor · *TGF-β* signaling

A. M. Adesina (✉) · Y. Nguyen · V. Mehta · H. Takei
Department of Pathology, Texas Children's Cancer Center, Baylor College of Medicine, One Baylor Plaza, Rm. 286A, Houston, TX 77030, USA
e-mail: aadesina@bcm.tmc.edu

P. Stangeby · S. Crabtree
Department of Pathology, University of Oklahoma Health Sciences Center, Oklahoma City, OK, USA

M. Chintagumpala
Division of Hematology-Oncology, Texas Children's Cancer Center, Baylor College of Medicine, Houston, TX, USA

M. K. Gumerlock
Department of Neurosurgery, University of Oklahoma Health Sciences Center, Oklahoma City, OK, USA

## Introduction

Medulloblastomas are the second most common malignant tumors in childhood with a frequency of about 1 in 200,000 children annually and accounting for about 20% of brain tumors in children. These tumors arise in the cerebellum, and are classified as embryonal tumors composed of small blue cells; a feature shared with other supratentorial primitive neuroectodermal tumors [1]. Insight into the underlying molecular mechanisms for the biology of medulloblastoma is beginning to emerge. In subsets of medulloblastoma, activation mutations involving important regulators of the sonic hedgehog and the Wnt pathway have been reported [2, 3]. Frequent chromosomal changes including isochromosome 17q with loss of variable regions

of 17p have also been documented. Although, the immunohistochemical detection of the expression of p53 gene protein has now been shown to be a poor prognostic marker in these tumors [4, 5, 6], mutations involving p53 gene, a gene located at 17p13.3, which is a locus often deleted in medulloblastomas or amplification of mdm2 gene (protein product binds p53) is uncommon, thus implicating other mechanism/s in the deregulation of p53 expression in medulloblastomas [6, 7, 8] Genomic amplification of the *MYC* oncogene or overexpression of the *myc* mRNA identifies a poor prognostic group of medulloblastoma. The close relationship between *MYC* oncogene amplification and the anaplastic /large cell histologic subset with a more aggressive phenotype is well documented [9, 10, 11]. CGH studies have identified specific genomic regions of amplification and deletion, and more recent correlations of these genomic alterations with gene expression profiling identify specific genetic and expression signatures that stratify the different histologic and prognostic groups of medulloblastoma [12, 13, 14]. In addition, conventional and array based CGH studies have shown genomic gains of a number of genes including *PIK3CA, PGY1, MET, ERBB2*, and *CSE1L* [15]. *ERBB2* overexpression has been associated with advanced metastatic disease and poor clinical outcome [16, 17] while *trk C* expression has been associated with the desmoplastic histology and better survival [18, 19]. Digital karyotyping has also been utilized for the identification of amplification of *otx2*; a homeobox gene located at 14q22.3 with important role in specification and regionalization of the forebrain and midbrain during early neurogenesis, and it shows a distinct correlation with the anaplastic phenotype [20, 21]. Many of the gene mutations and oncogene amplifications described above represent progression events associated with subsets of aggressive medulloblastomas. There is very little understanding of the initiating events in the development of medulloblastoma. Efforts at identifying initiating events have been focused on genetic syndromes such as nevoid basal carcinoma syndrome due to the *ptch* gene mutation [22], Turcot's syndrome with APC mutation [23] and Li-Fraumeni syndrome with *p53* germ line mutations [24] all of which have been associated with medulloblastoma. The observation of the development of medulloblastoma in only a subset of the *ptch* mutation *(ptch–/–)* mice, even though all mice possess the same genetic predisposition suggests that other genetic event/s that influence susceptibility to medulloblastoma exist. One would expect that such an event would be present in a large proportion of medulloblastomas and of necessity in all histologic types of medulloblastoma. Using conventional and BAC array CGH, we have identified another 14q genetic event, a 14q12 amplicon, distinctly separate from the previously reported *otx2* at 14q22.3 [20, 21] which includes the *FOXG1* gene. *FOXG1* copy gain was first observed by aCGH and confirmed by Qrt-PCR in 9 out of 9 analyzed medulloblastomas and by Qrt-PCR in 93% (55/59) of a validating subset of medulloblastomas. We demonstrate the increased expression of *FOXG1* as detected by immunohistochemistry with *FOXG1* specific antibody, as well as an inverse relationship between *FOXG1* expression and the expression of *p21cip1* in these medulloblastomas. *FOXG1* has been implicated in the repression of *TGF-β* induced expression of *p21cip1* [25]. Our findings are consistent with such a role for *FOXG1*. *TGF-β* is produced in the cerebellum and plays an important role in the elimination of neuronal precursor cells that do not establish neuronal connections. It also cooperates with *BDNF* to inhibit cellular proliferation in the cerebellum. We hypothesize that the deregulation of *FOXG1* by gene copy gain and amplification may represent an early event upon which all other reported medulloblastoma subset specific mutations or genetic events resulting in deregulation of critical signaling pathways are superimposed for the development and progression of medulloblastoma. This is the first report of a role for *FOXG1* in the pathogenesis of medulloblastoma.

## Methods

### Medulloblastoma tumors

Nineteen (19) medulloblastomas from the files of the Department of Pathology, University of Oklahoma Health Sciences Center, Oklahoma City were analyzed in this study. A validating set of 64 medulloblastomas were retrieved from the files of the Department of Pathology, Texas Children's Hospital, Houston TX. Four of these medulloblastomas did not have enough tissue for immunohistochemical studies while 5 cases (including the four cases) did not have sufficient tissue for molecular studies, leaving a total of 60 cases for immunohistochemistry and 59 cases for molecular studies. The research protocol was approved and carried out in accordance with the guidelines of the Institutional Review Board, University of Oklahoma Health Sciences Center and Institutional Review Board, Baylor College of Medicine, Houston, Texas. Histologic sections from all tumors were reviewed and were classified according to the World Health Organization's histologic classification (WHO) of medulloblastoma (Table 1 and 2).

### DNA extraction, CGH, post-hybridization scanning and analysis

Genomic DNA was extracted from paraffin embedded tumor tissue using the Qaigen kit (Qiagen, Valencia, CA)

**Table 1** Result of genomic gains and losses by conventional CGH: [ ] denotes events observed in one hybridization with only a trend in the same direction of deletion or gain in the dye swap

| Tumor ID | Histology | Losses | Gains | BAC array CGH |
|---|---|---|---|---|
| ML1 | Classic | 16q11.1–12.1 | 5, 7q33–36, 7p22, 8p23.3, 8q24.1–24.3, 17q25 | Yes |
| ML2 | Desmoplastic | None | 1q43–44, 3q13.3–29, 3p26, 5p15.2–15.3, [7p11.2–13], [8q24.3], 9p23–24, [18p11.3] | No |
| ML5 | Desmoplastic | None | 3q21–29 | No |
| ML6 | Classic | 13q11–22, 16q23–24, 17p12–13 | 1q31–32, 2p16–25, 12q14–23, 13q32–34, 17q21.3–25 | Yes |
| ML9 | Classic | 17p12–13 | 2q24–31, 3p12, 4q33–34, [6q14–22], 11q22–25, [13q14–22], [13q33–34], 17q21–25, 18p11.3 | Yes |
| ML10 | Desmoplastic | None | 7p22, 10p14–15, 18p11.3 | No |
| ML11 | Classic | None | 4q13, 17q11.2–25 (all of q), 18p11.3 | No |
| ML12 | Desmoplastic | 10q22–26 | 1p12–13, 3p12, 4p13, 5p12–14, 6q12–14, 13q12, 14q11.2, 15q11.2, 16q12.1–12.2, 21q11.2–21 | Yes |
| ML13 | Desmoplastic + Classic | [10q24.3–26.3], [17p13] | 2p22–25, 4p15.3–16, 5p15.2–15.3, 7p13–22, 7q33–36, 12q22–24.3, 16p11.2, [16q11.1–12.2], [16p11.1], 17q21.3–25 | Yes |
| ML16 | Medullomyoblastoma | 17p12–13 | 7q11.2–36, 17q11.2–25 (all of q), 18q11.2, 18q22–23 | Yes |
| ML17 | Classic | 17p12–13 | 17q21–25, [18p11.3] | Yes |
| ML18 | Classic | 17p12–13 | 2q24–32, [17q all] | No |
| ML19 | Classic | 7q21–36 | 11q23–25, [17q22–25] | Yes |
| ML20 | Classic | 17p12–13 | Chr 4 all, 17q12–25 | No |
| ML21 | Classic | 10q11.2–22, 11p11.2–13, 11q12–24, 16q13–24 | 2q22–33, 2p24–25, 3q29, 4q12–22, 4q34–35, 4p13–15.1, 5p13–15.3,5q11.2–13, chr 7 all, 12p11.2–13, 12q15–21,14q11.2–32 (all of q), | Yes |
| ML22 | Classic | [16q23–24] | 1p11–13, 1q11–12, 3p11–12, 3q11.1–11.2, 5p11–14, [5q13–31], 6q11–22, 12p11.1–12, [12q12–13], [12q15–21], [13q21–22], 16q11.1–12.2, 17p13, [17q25], 18 p all, 18q11.1–21 | No |
| ML24 | Desmoplastic | None | None | No |
| ML25 | Classic | None | 1q31–44, chr 6 all, 8q22, 8q24.3 | No |

and the manufacturer's protocol. Reference DNA was obtained from paraffin embedded tonsillar tissue of normal male and female, respectively. For chromosomal CGH, the test DNA was chemically labeled in a standard nick translation reaction substituting dTTP by Spectrum Green dUTP (Vysis) while the reference (normal) DNA is labeled substituting dTTP by Spectrum Red dUTP (Vysis). The DNase 1 concentration in the labeling reaction was adjusted to give an average fragment length within 300–2000 bp. The labeled probes were separated from unincorporated nucleotides by Sephadex columns. A 1:1 mixture of test and reference DNA (120–200 ng each) was precipitated in ethanol in the presence of 10 μg of COT-1 DNA (Gibco-BRL, Gaithersburg, MD), dissolved in 10 μl of hybridization solution (50% formamide, 2× SSC, and 10% dextran sulfate), and denatured at 73°C for 5 min. The probe mixture was then applied to target normal metaphase preparations which have been denatured at 73°C for 5 min in 70% deionized formamide in 2× SSC and dehydrated through an ethanol series of 70, 90 and 100% ethanol. Hybridization occurred at 37°C for 4 days. Post-hybridization washes comprise sequential washes with 50% formamide in 2× SSC at 43°C (3× washes for 5 min each) followed by 2× SSC/0.1%NP 40 at 43°C (3× washes for 5 min each). Chromosomes were identified by means of the banding appearance produced by staining with 4,6-diamino-2-phenylindole 2-HCl (DAPI) at 80 ng/ml in an antifade (Citifluor) solution. The fluorescence signals from the hybridization were captured and analyzed using the Applied Imaging Cytogenetic Workstation image analysis equipment and Genus software.

For BAC array CGH, DNA samples for tumor and reference were fragmented by digesting with *Eco*R1 and concentrated using the Zymo Research's DNA Clean and ConcentratorTM-5. An aliquot was run on 1% agarose electrophoresis gel to confirm adequate fragmentation. DNA concentration was determined using the Agilent Nanodrop™ Spectrophotometer. 500 ng of reference and

**Table 2** Result of *FOXG1* immunostaining in validating set of medulloblastomas

| ML | Diagnoses | FOXG1 (I) | FOXG1 (E) | ML | Diagnoses | FOXG1 (I) | FOXG1 (E) |
|---|---|---|---|---|---|---|---|
| 1_HT | Focal nodular + Anaplastic | ++ | +++ | 35_HT | Large cell | +++ | ++++ |
| 2_HT | Classic | ++ | ++++ | 36_HT | Nodular | + | + |
| 3_HT | Classic+focal nodular | +++ | +++ | 37_HT | Classic | +++ | ++++ |
| 4_HT | Classsic+focal nodular | ++ | ++ | 38_HT | Anaplastic | 0 | 0 |
| 5_HT | Large cell+focal nodular | + | ++ | 39_HT | Anaplastic | +++ | +++ |
| 6_HT | Anaplastic+focal nodular | ++ | +++ | 40_HT | Anaplastic | + | +++ |
| 7_HT | Large cell | ++ | +++ | 41_HT | Classic | ND | ND |
| 8_HT | Nodular +anaplasia | + | ++ | 42_HT | Nodular+Anaplastic | + | ++ |
| 9_HT | Anplastic/large cell | + | +++ | 43_HT | Classic + Nodular +Focal Anaplastic | + | ++ |
| 10_HT | Nodular | ++ | ++ | 44_HT | Anaplastic/large cell | ++ | ++ |
| 11_HT | Nodular | + | ++ | 45_HT | Classic | + | ++ |
| 12_HT | Anaplastic | + | + | 46_HT | Nodular | ++ | +++ |
| 13_HT | Nodular | +++ | +++ | 47_HT | Anaplastic | ++ | +++ |
| 14_HT | Classic | ++ | +++ | 48_HT | Nodular | ++ | +++ |
| 15_HT | Nodular | +++ | ++ | 49_HT | Nodular | ++ | +++ |
| 16_HT | Classic | ++ | ++ | 50_HT | Classic | +++ | +++ |
| 17_HT | Classic | ++ | ++ | 51_HT | Classic | ++ | +++ |
| 18_HT | Anaplastic/large cell | ++ | ++ | 52_HT | Classic | ND | ND |
| 19_HT | Nodular | + | ++ | 53_HT | Anaplastic | ++ | ++ |
| 20_HT | Nodular | + | ++ | 54_HT | Anaplastic | ++ | +++ |
| 21_HT | Classic | + | + | 55_HT | Anaplastic | +++ | +++ |
| 22_HT | Anaplastic | + | + | 56_HT | Nodular | ++ | ++ |
| 23_HT | Nodular/anaplastic | ++ | +++ | 57_HT | Anaplastic/large cell | +++ | +++ |
| 24_HT | Nodular | + | ++ | 58_HT | Classic | ++ | +++ |
| 25_HT | Classic | + | ++ | 59_HT | Classic+anaplastic | ++ | ++ |
| 26_HT | Classic | ++ | +++ | 60_HT | Anaplastic | ++ | +++ |
| 27_HT | Nodular | +++ | +++ | 61_HT | Anaplastic | ++ | ++++ |
| 28_HT | Nodular | + | + | 62_HT | Anaplastic | + | + |
| 29_HT | Classic | ++ | +++ | 63_HT | Nodular | ++ | +++ |
| 30_HT | Large cell /anaplastic | ++ | ++++ | 64(34)_HT | Classic | ++ | ++ |
| 31_HT | Classic | + | ++ | 65_HT | Classic | ND | ND |
| 32_HT | Classic | + | + | 66_HT | Nodular/anaplastic | +++ | +++ |
| 33_HT | Classic | ++ | ++ | | | | |

The immunostained sections were graded semi-quantitatively for intensity [I] (0, negative; or 1 to 3+) as well as extent [E] (0%: 0, ≤ 25%: 1+, 26–50%: 2+, 51–75%: 3+, >75%: 4+) of staining. There is a statistically significant positive correlation between protein expression and *FOXG1* copy number (Spearman's rank order correlation coefficient = 0.276; $P = 0.038$). in these medulloblastomas

tumor DNA were differentially labeled with Cy3-dCTP and Cy5-dCTP by random primer labeling method using the Bioprime labeling kit (In vitrogen). An aliquot was run on 1% agarose electrophoresis gel to ensure synthesis of DNA fragments averaging 100 bp. Test and reference DNA were denatured, mixed and hybridized to BAC array slides (Spectral Genomics). Following 16 hour incubation at 37°C, post-hybridization washes were carried out at 50°C in 2× SSC, 50% Formamide × 20 min, 2X SSC, 0.1% Igepal × 20 min, and 0.2× SSC × 10 min. Two rapid washes (5 s each) in double distilled water were carried out at room temperature followed immediately by blowing the slides dry with a stream of nitrogen gas. Slides were scanned and analyzed using ScanArray (Perkin Elmer) and SpectralWare™ software. The BAC array slide (Spectralchip™ 2600) provides a microarray-based molecular comparative genomic hybridization using 2,632 clones spanning across the genome at one megabase (1 MB) intervals on the average with clones mapped to a cytogenetic linear position.

Quantitative real time polymerase chain reaction (Qrt-PCR):

Copy number of *FOXG1* gene in the genomic DNA from each medulloblastoma tumor was determined by Qrt-PCR. PCR reactions containing genomic DNA and SYBR® GREEN PCR Master Mix (Applied Biosystems) and primers for *FOXG*1 were performed for 30 cycles in triplicate. Primers were designed using the Applied Biosystems primer design program for *FOXG1*; F-CCTG CTGGCTCAGAAATGC; R-GAGGCGA GGCACTACT TCC and *PRDK1* F-TGCTGCAAGTAAAAATGAGAA AGC; R-CATTCAACTAGAA CTCAGTGATTATTG. Amplification products were verified by agarose gel electrophoresis and melting curves. DNA amplification was normalized internally to *Albumin* gene, relative to control normal human genomic DNA from peripheral blood lymphocytes. We chose to use the *Albumin* gene as reference control for Qrt-PCR instead of a reference locus on chromosome 14 because (1) we did not want to miss tumors with polysomies for chromosome 14, and (2) polysomies or copy gains/amplification involving the *Albumin* gene locus at 4q13.3 have not been reported in medulloblastomas.

Immunohistochemistry for *FOXG1* and *p21cip1*

5 μm thick sections were obtained from formalin-fixed paraffin embedded sections of representative sections of the validating set of medulloblastomas. The tissue sections were deparaffinized in Xylene, followed by graded hydration in 100% and 70% ethanol to $H_2O$. Antigen retrieval was done by boiling in 10 mM EDTA × 25 min. Endogenous peroxidase was blocked with 3% $H_20_2$/Methanol × 15 min, then incubated with 20% goat serum × 20 min. Sections were incubated with 1:20 dilution of polyclonal anti-*FOXG1* antibody (Abcam Inc, Cambridge, MA) × 1 h at room temperature or anti-p21cip1 antibody overnight at 4°C (DAKO). This was followed by incubation with anti-rabbit secondary antibody conjugated with HRP × 30 min. DAB was used as color reagent. The secondary antibody was conjugated with FITC for immunofluorescence staining. Fetal kidney showing nuclear positivity in the proximal and distal renal tubules served as control. The immunostained sections were graded semi-quantitatively for intensity (I) (0, negative; or 1 to 3+) as well as extent (E) (0%: 0, ≤ 25%: 1+, 26–50%: 2+, 51–75%: 3+, >75%: 4+) of staining.

Transfection with *FOXG1* specific siRNA

DAOY, a medulloblastoma cell line was obtained from the American Type Culture Collection *(ATCC, Manassas, VA)* and propagated in Dulbeco's Minimum Essential Medium (DMEM) supplemented with 10% fetal calf serum. Cells were transfected with *FOXG1* specific siRNA using siPortamine and recommended protocol (Catalog # 115630, Applied biosystems). GAPDH specific siRNA and Luciferase gene specific siRNA served as positive and negative transfection controls, respectively.

MTT proliferation assay

MTT [3-(4,5-dimethylthiazol-2-yl)-2,5-diphenyltetrazolium bromide] assay is based on the ability of a mitochondrial dehydrogenase enzyme from viable cells to cleave the tetrazolium rings of the pale yellow MTT and form a dark blue formazan crystal which is largely impermeable to cell membranes, thus resulting in its accumulation within healthy cells. Solubilization of the cells by the addition of a detergent results in the liberation of the crystals which are solubilized. The number of surviving cells is directly proportional to the level of the formazan product created. The color was quantified using a simple colorimetric assay. The results were read on a multi-well scanning spectrophotometer (ELISA reader). The MTT Cell Proliferation Assay *(ATCC, Manassas, VA)* measures the cell proliferation rate and conversely, when metabolic events lead to apoptosis or necrosis, the reduction in cell viability. The MTT reagent yields low background absorbance values in the absence of cells. For each cell type the linear relationship between cell number and signal produced is established, thus allowing an accurate quantification of changes in the rate of cell proliferation. 10 μl of MTT Reagent is added to each well (96 well plate), including controls. Plate is returned to cell culture incubator for 2–4 h. Periodically the cells are viewed under an inverted microscope for presence of intracellular punctate purple precipitate. When the purple precipitate is clearly visible under the microscope, 100 μl of detergent reagent is added to all wells, including controls. The plate is gently swirled without shaking. Plate is left with cover in the dark for 2–4 h or overnight at room temperature. Plate cover is removed and the absorbance in each well is measured, including the blanks, at 570 nm in a micro-titer plate reader. Average values are determined from triplicate readings from which are subtracted the average value for the blank. The number of cells is determined from a previous plot of absorbance against number of cells/ml.

## Results

CGH analysis

The chromosomal identification in each tumor karyotype was verified. The pattern of chromosomal gains and losses

from the cCGH analysis of the initial 19 medulloblastoma tumors were automatically generated by the Applied imaging software with a cut off value of test to reference ratio of 0.8 for a deletion event and 1.2 for a copy gain event. The ratios for each chromosomal region in a tumor represents an average of about 20–30 chromosomes from 10 to 15 metaphase spreads. The events were accepted as definite when present in the initial run and in the dye swaps. Events above 1.2 or below 0.8 in the initial run but with a strong tendency towards the cut off value in the dye swap were identified as possible but not definite events. A summary of the pattern of losses and gains in the tumor set is shown in Table 1. The commonest deletion event involved 17p and was present in 5 out of 19 (26.3%) tumors. Less frequent deletions were seen at 16q, 10q, 11p, 11q and 13q. 6 out of 19 tumors (31.6%) did not show any detectable deletion. 4 out of the six tumors with no deletions were desmoplastic tumors while the other two tumors were classic tumors. A regression analysis of the frequency of deletions versus survival showed a negative correlation with $P = 0.02$ and $r^2 = 0.3496$. The commonest gain involved 17q and was seen in 9 out of 19 (47.4%) tumors. Less frequent gains were seen at 1p, 1q, 2p, 2q and 14q. 2p gain was present in 3 out of 19 tumors and the region of gain encompassed variable segments from 2p16 to 2p25 and in these three tumors included the *n-myc* locus.

Nine (9) out of nineteen (19) tumors with frequent genetic events by cCGH analysis were further analyzed by aCGH. aCGH is a more sensitive technique for genome wide scanning and for the detection of deletion or gain events in the genome. The scanned images of hybridized arrays were analyzed using Spectral Genomics software. This software normalizes the scanned image data using a ''global'' method [26] of normalization and identifies a probe locus as showing a gain or deletion if the ratio of the tumor DNA to the reference control normal DNA is greater than 1.2 or less than 0.8 in both the initial run and dye swaps for each tumor. Comparable analysis using Lowess' method [27] of normalization showed values similar to those of the global method. Probe spots where the initial run and the dye swap show divergent values such that the initial run shows a ratio above 1.2 while the dye swap shows a ratio less than 0.8 were rejected. The $\log_2$ ratios for each probe spot/tumor were also analyzed using the Agilent CGH analytics 3.1 software. Analysis of copy gains and losses revealed multiple loci in the genome of medulloblastoma tumors with low levels of copy gain and deletions. The composite of genetic events identified from the analysis of these nine medulloblastomas by aCGH is shown in Fig. 1. The most frequent sites of genomic gains were 14q (67%), 17q (33%), 7 (33%) and 12q (33%). Less frequent gains were seen at 5q (22%) and 2p (22%). The most frequent genomic deletions were at 16q (56%), 17p (44%) and 5q (33%). Less frequent deletions were at 10q (22%), 8p (22%) and 13q (22%).

## Quantitative real time PCR (Qrt-PCR)

For validation of observed gains and deletions from aCGH, the genomic DNA of the tumors was subjected to Qrt-PCR. To determine which genes are potentially affected at 14q12 (the locus with the most frequent gain by aCGH), the BAC probe at the 14q12 locus was identified as RP11-125A5. Potential involved genes localized to the 14q12 chromosomal region with overlap or proximity to the BAC—RP11-125A5 were identified using the UCSC browser (www.genome.ucsc.edu). The two genes closest to the gained BAC probe (Fig. 2A) which mapped to this region, *FOXG1* and *PRKD1* (*PRKCM*) were subjected to Qrt-PCR. Copy gain of *FOXG1*, a gene mapping centromeric to the gained BAC probe was evident in 9 out of 9 tumors (Fig. 2B). On the other hand, allelic deletion for *PRKD1*, a gene mapping telomeric to the gained BAC probe was seen in 7 out of the 9 tumors. Values represent triplicate runs for each tumor and were confirmed in repeat runs of the Qrt-PCR.

To validate the frequency of copy gain involving *FOXG1* in medulloblastoma, a total of 59 out of a validating set of 60 medulloblastomas had sufficient genomic DNA available to be used as a validating subset of tumors. They were subjected to Qrt-PCR under the same conditions as described. 93% (55/59) of these medulloblastomas were found to have multiple copies (2–21 fold) of the *FOXG1* gene. 64.4% (38 out of 59) of the tumors with multiple copies had ≥ 5 copies consistent with gene amplification (Fig. 3), thus representing a frequent genetic event in this subset of medulloblastoma.

## Immunohistochemical analysis for *FOXG1*

Expression of *FOXG1* was assessed by immunohistochemistry in normal cerebellum and medulloblastoma. In normal cerebellum, *FOXG1* expression was absent in the nuclei of the internal granular neurons and Purkinje cells (Fig. 4F). Fetal kidney was noted to have a robust expression of *FOXG1* in the developing proximal and distal renal tubules and it served as the immunohistochemistry positive control tissue. In medulloblastomas, *FOXG1* protein was detected in the nuclei of 59 of 60 validating tumors. Since *FOXG1* is not expressed in normal cerebellum, its expression in medulloblastoma represents aberrant expression. *FOXG1* protein expression was demonstrated as follows: mild (+) in 20/60 (33%); moderate to marked (++/+++) in 39/60 (65%); 1 tumor (2%) was negative. The positively staining nuclei were widely distributed in the tumors (Fig. 4A–C and E). *FOXG1* protein was

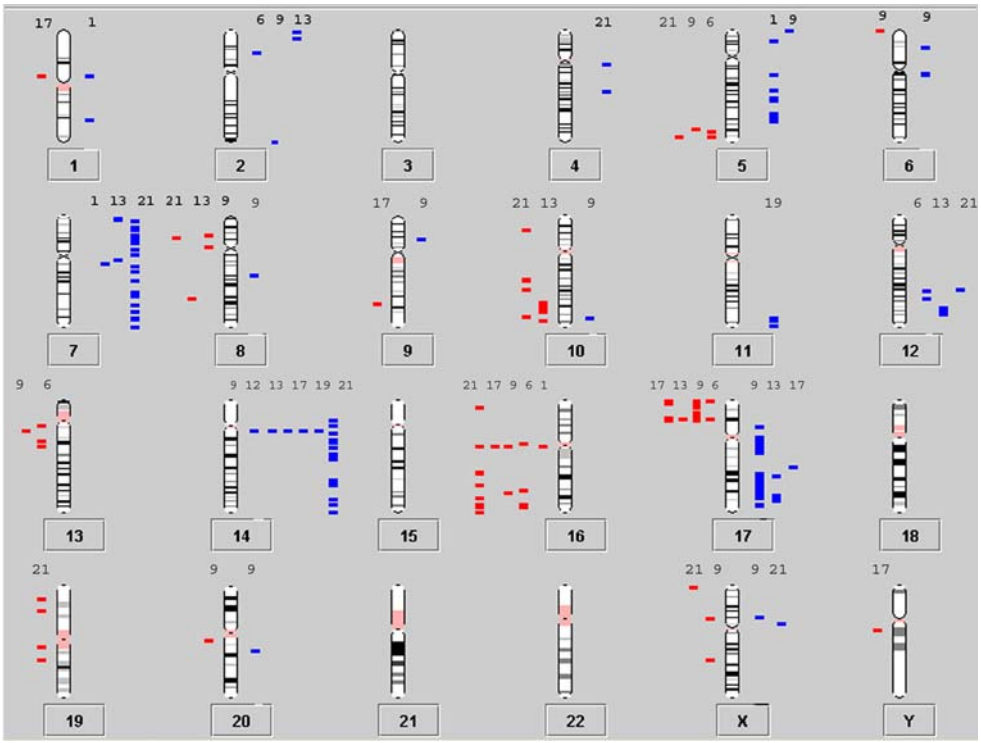


**Fig. 1** Summary composite ideogram for BAC array CGH analysis: Nine [9] test medulloblastomas showing the frequency of distribution of genetic changes including regions of genomic deletions (red) and gains (blue). Frequent deletions for 17p and 16q, frequent gains for 14q12, and occasional trisomies for chromosomes 5, 7, 14 and 17q are present

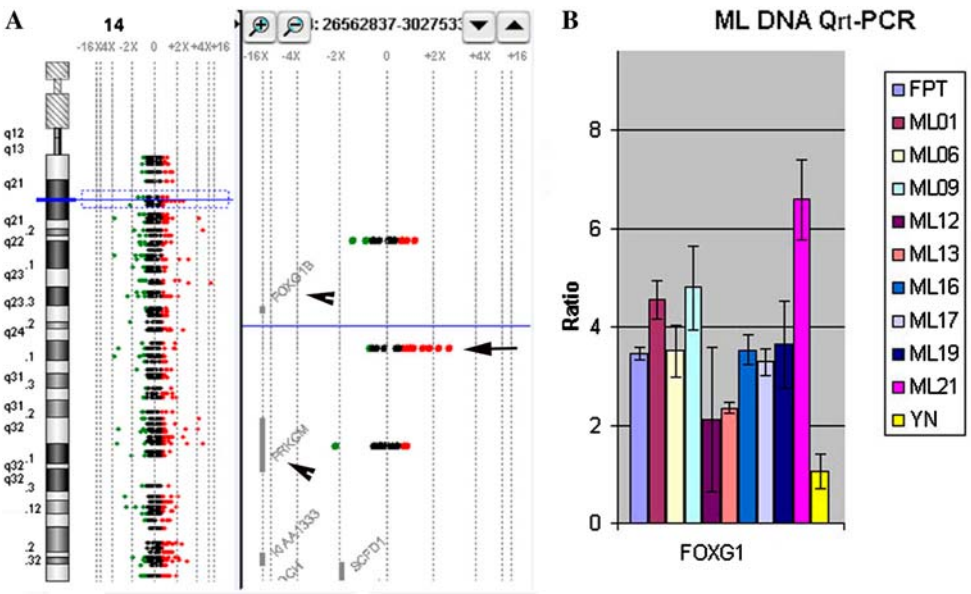


**Fig. 2** (**A**) Ideogram of the 14q12 locus (RP11–125A5): It shows high frequency of gain (6/9) at this locus. Chromosome 14 linear position 26.5 M to 30.27 M, approximately [enclosed in the blue rectangle (broken lines)] is enlarged to the right of the ideogram and shows the localization of the RP11–125A5 BAC (arrow). The genes closest to this BAC in this ''zoomed in'' image based on the human genome assembly 17 are centromeric *FOXG1* and telomeric *PRKD1 (PRKCM)* (arrow heads) (**B**) Qrt-PCR on genomic DNA for FOXG1: Nine test medulloblastoma tumors show 2 to 7 fold gain in *FOXG1* gene copy number in all tumors

detectable in desmoplastic (nodular), classic, as well as, anaplastic / large cell histologic subtypes (Table 2). An inverse relationship was noted between the expression of *FOXG1* and *p21cip1* (Fig. 4C and D) consistent with a negative regulation of *p21cip1* expression in most of these tumors. *FOXG1* copy gain (>2 to 21 folds) showed a significant positive correlation with protein expression (Spearman's rank order correlation coefficient = 0.276; $P = 0.038$).

## In vitro modulation of *FOXG1* effect using *FOXG1* specific siRNA

The medulloblastoma cell line, DAOY was used for in vitro experiments. Copy gain of *FOXG1* gene and expression were determined by Qrt-PCR and Qrt-RT-PCR respectively. A five fold copy of the *FOXG1* gene and $2 \times 10^3$ fold upregulation of the expression of the *FOXG1* mRNA was observed (Fig. 5A). A two-fold copy gain of

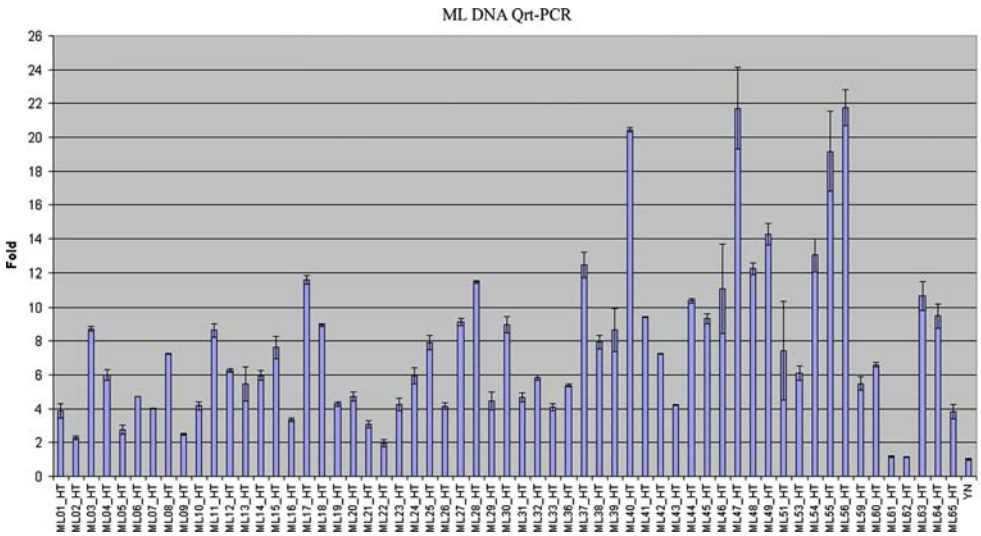


**Fig. 3** Qrt-PCR on genomic DNA of validating medulloblastomas: 59 out of 60 tumors in the validating set of medulloblastomas show a 2–21 fold gain in *FOXG1* gene copy number in 93% (55/59) of tumors. 64.4% (38/59) of tumors have ≥ 5 fold gain in gene copy number. Human normal peripheral blood lymphocyte genomic DNA (YN) served as control. Values represent the mean of triplicate runs for each tumor. Repeat triplicate runs confirm result

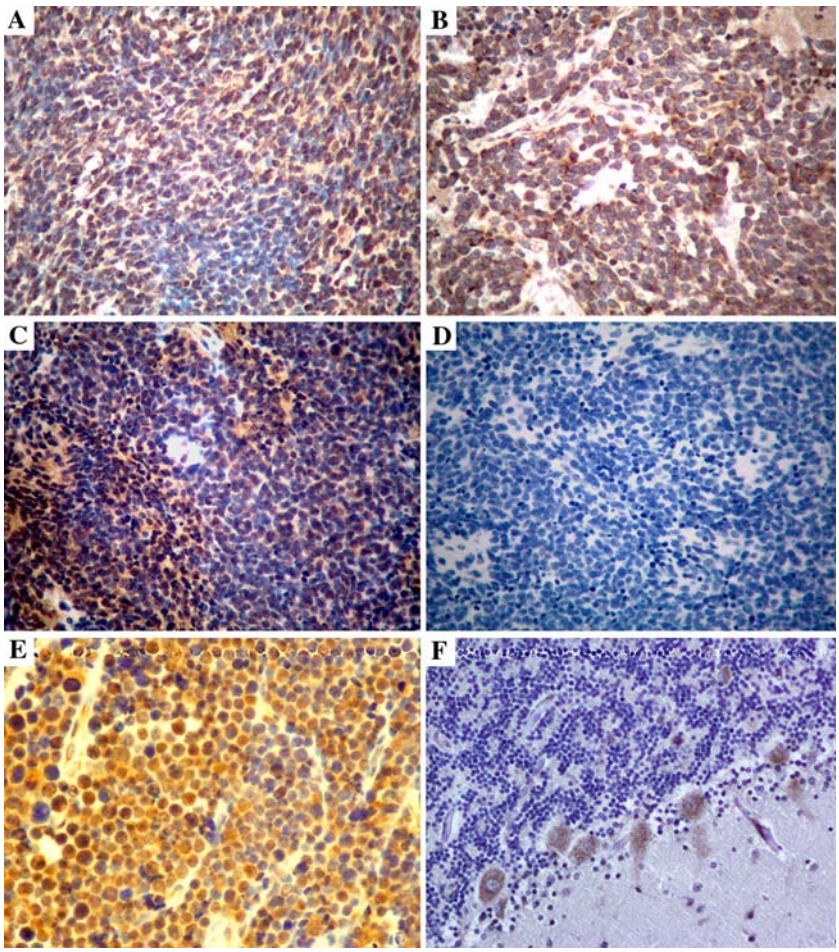


**Fig. 4** Immunostaining for *FOXG1* and *p21cip1* in medullblastomas: Medulloblastomas show variable diffuse and intense nuclear positivity for *FOXG1* (**A**, **C**, **E**), a rare perinuclear dot-like pattern of staining for *FOXG1* (**B**) and negative nuclear staining for p21cip1 (**D**). Figures C and D are from the same tumor. Mature cerebellum shows no demonstrable nuclear positivity for *FOXG1* in internal granular neurons or Purkinje cells (**F**) [**A**–**D** and **F** × 200; **E** × 400].

the *FOXG1* gene and a $4 \times 10^3$ fold upregulation of the expression of the *FOXG1* mRNA was also observed in D283-Med. Following treatment of DAOY with *FOXG1* specific siRNA (Catalog # 115630, Applied biosystems), a 65–70% ''knockdown'' of *FOXG1* mRNA expression (Fig. 5B) was accompanied by a 23% reduction in proliferation rate (Fig. 5C). Other *FOXG1* specific siRNA (Catalog # 6439 and 145145, Applied biosystems) showed similar *FOXG1* knockdown efficiency (data not shown). The presence of 0.1 ng/ml of *TGF-β* augmented the

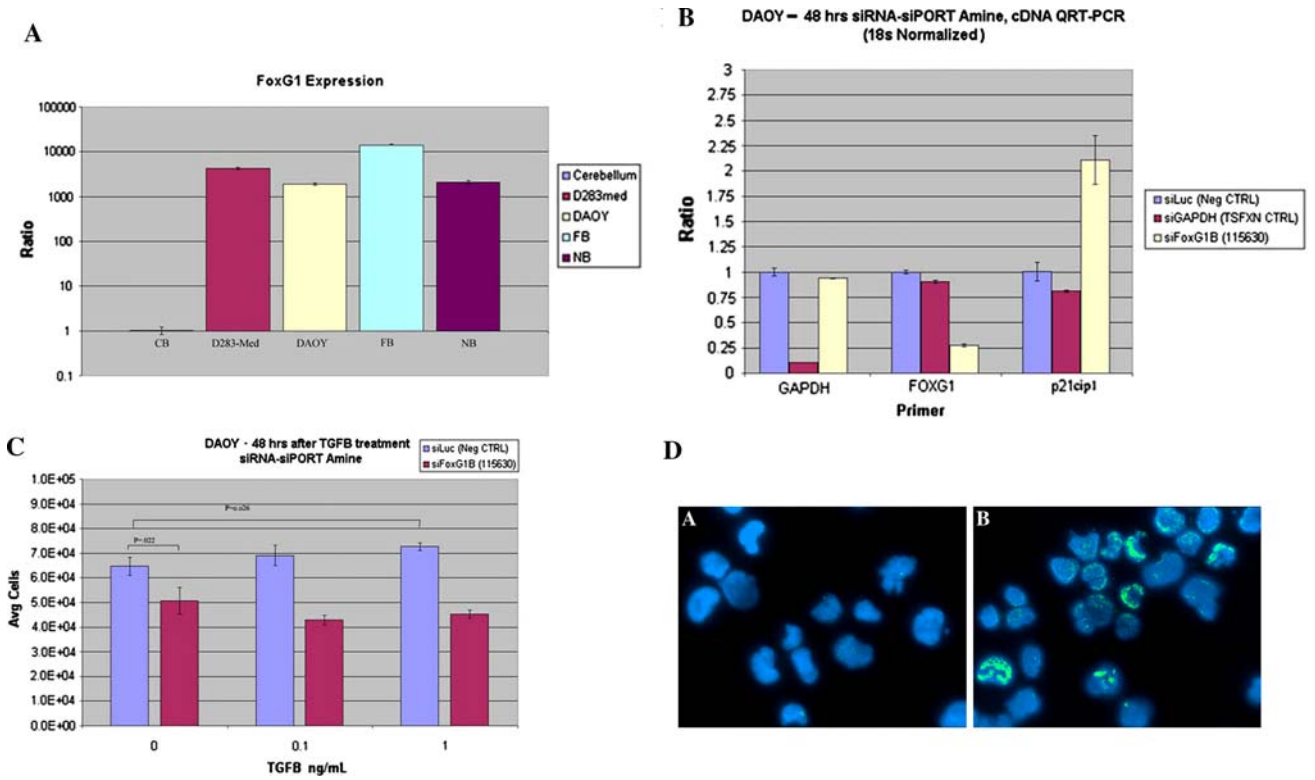


**Fig. 5** (**A**) Qrt-RT-PCR for *FOXG1* in medulloblastoma cell lines: High levels of expression of *FOXG1* are seen in DAOY (~$2 \times 10^3$ fold) and D283Med (~$4 \times 10^3$ fold) when compared with normal cerebellum. Levels are comparable to those seen in Fetal Brain (FB) and Normal adult cerebral cortex (NB). (**B**) Transfection of DAOY cells with *FOXG1* specific siRNA: It shows a 65–70% inhibition of *FOXG1* mRNA and a 2 fold upregulation of *p21cip1* expression. Cells transfected with nonspecific *Luciferase* gene siRNA served as negative controls and do not show any evidence of ''knockdown''of *FOXG1* mRNA or *GAPDH* mRNA. Cells transfected with siRNA to *GAPDH* served as positive controls for the transfection protocol and show a more efficient ''knockdown ' of GAPDH mRNA when compared with *FOXG1* mRNA ''knockdown'' by *FOXG1* specific siRNA. This is consistent with variable efficiency of transfection of siRNA for different genes. (**C**) MTT assay for cell proliferation: There was a 23% decrease in proliferation index ($P < 0.05$) which further decreased by 39% in the presence 0.1 ng/ml of *TGF-β*. Note paradoxical increase in proliferation index in the absence of *FOXG1* inhibition ($P < 0.05$). (**D**) Immunofluorescence for p21cip1 following siRNA treatment of DAOY: Cells transfected with (**A**) *Luciferase* gene specific siRNA as negative control, do not show demonstrable increase in expression of p21cip1, while in (**B**) *FOXG1* specific siRNA transfection shows upregulation of expression of p21cip1. The variable expression between cells is consistent with variable transduction in individual cells [all × 400]

reduction in proliferation index to 39%. Immunofluorescence staining with *p21cip1* specific antibody shows upregulation of *p21cip1* protein in DAOY cells treated with *FOXG1* specific siRNA (Fig. 5D). The upregulation of *p21cip1* seen in the DAOY cells examined by immunofluorescence is variable and reflects variable efficiency of transfection of individual cells with the siRNA. Using Qrt-RT-PCR, a 2-fold upregulation of *p21cip1* mRNA following siRNA transfection was demonstrated (Fig. 5B).

## Discussion

This report documents for the first time, the dysregulation of *FOXG1* in medulloblastoma with frequent gene copy gain and aberrant protein expression in all histologic types of medulloblastoma and in 93% of our cases of medulloblastoma. It suggests that dysregulation of *FOXG1* is a significant and possibly early event in the development of medulloblastoma. We hypothesize that overexpression or aberrant expression of *FOXG1* in the precursor stem cells of medulloblastoma would maintain these cells in the undifferentiated state and also prevent their response to normal programmed cell death, thereby setting the stage for additional progression related genetic events associated with neoplastic transformation. *FOXG1* is known for its role in neurodevelopment [28–30] and has been shown to reduce the responsiveness of cells in vitro to growth inhibition by *TGFβ*. Members of the *TGF-β* superfamily including *TGF-β1, β2 and BMP2, 4* and *7* also play significant roles during the development of the CNS. *TGF-β2* and *BDNF* have been implicated in the maintenance of an antiproliferative microenvironment in the normal cerebellum [31]. *TGF-β1* has been shown to selectively increase

the expression of *p21cip1* in the ventricular zone (VZ). A decrease in the fraction of ventricular zone (VZ)-cycling cells by 21% was found to be associated with an increase in the number of VZ cells exiting the cell cycle by 24%. In addition, high *p21cip1* expression levels were observed in VZ cells as they exited the cell cycle [32]. *Beta catenin* expression is associated with sequential expression of *BMPs 2, 4, 7* resulting in neuronal development as well as gliogenesis [33]. A recent study has reported better survival in medulloblastomas with activated (mutated) *β catenin* [34]. This observation was unexpected and is counterintuitive. Whether this observation in medulloblastomas is due to the antiproliferative effects of *BMPs* induced by *β catenin* remains to be determined. Paracrine *TGF-β2* mediated activation of the *Smads 2* and *4* also have anti-proliferative effects on the mature cerebellum by upregulating the expression of *p21cip1* and *p27kip1* in the cerebellum. In addition, cerebellum-derived *BDNF* via *ERK1/2* signaling augments *TGF-β2* synthesis / secretion into the cerebellar microenvironment, thereby enhancing the anti-proliferative effects of *TGF-β2* in the cerebellum [31].

*FOXG1* expression has been shown to be sufficient to overcome the ability of *TGF-β* to block cells released from contact inhibition from re-entry into the cell cycle. These effects are mediated through the binding of *FOXG1* with *smad-FOXO* transcriptional complexes [35, 36]. In vivo studies suggest that *FOXG1* activity may not be primarily directed at inducing cell proliferation bu*t* may play a role in maintaining the undifferentiated state in order to properly time neurogenesis and allow the progenitor population sufficient time to expand, thereby delaying early cortical cell fate [37]. In essence, *FOXG1* is a transcriptional repressor that protects neuroepithelial progenitor cells from cytostatic and differentiation inducing signals [38, 39]. *FOXG1* expression is restricted to the neuroepithelial progenitor population that comprises the telencephalon in the developing mouse [40], and it is essential for forebrain formation [38]. Furthermore, excess *FOXG1* expression in vivo is associated with neural progenitor cell overgrowth; an effect requiring DNA-binding and repressor activity [41]. *FOXG1* is expressed at very low levels in normal cerebellum. We are not able to detect *FOXG1* in the differentiated cerebellum. A comparison of medulloblastoma cell lines DAOY and D283-Med with differentiated normal cerebellum shows upregulation of *FOXG1* expression to about $2 \times 10^3$ and $4 \times 10^3$ folds, respectively. These high levels (compared with normal cerebellum) in these medulloblastoma cell lines suggest that *FOXG1* expression in cerebellum derived medulloblastoma tumors and cell lines is an aberrant expression with possible role in neoplastic transformation. Available reports suggest that rather than directly affecting cell proliferation, mechanisms for *FOXG1* mediated overgrowth involve counteracting signaling induced by cytostatic factors of the *TGF-β* superfamily, including *TGF-β* and *BMP*. This is achieved through the repression of the transcription of cyclin dependent kinase inhibitors *p15Ink4b/p21cip1* and by reducing the frequency of normal programmed cell death or apoptosis [25, 35, 41]. An alternative mechanism for opposing *TGF-β* induced signaling involves hyperactive *PI3K* pathway that may also inhibit *TGF-β* induced cytostasis by activating an *akt*-mediated phosphorylation of the *FOXO1, 3* and *4* proteins with an exclusion of the *FOXO* proteins from the nucleus, thereby disrupting the *Smad-FOXO* transcriptional complex formation (Fig. 6) [39].

An immunohistochemical study of medulloblastomas shows increased expression of insulin growth factor-1 *(IGF-1)* and downstream proteins of the *PI3K-akt* pathway in medulloblastoma [42]. Overexpression of *IGF-2* has also been shown to enhance tumor development in the *ptch* mutation mice. In this study, *Shh*-induced tumor formation was enhanced by coexpression with *IGF2* and a*kt* with neither *IGF2* nor *Akt* causing tumors when expressed independently. Interestingly, the induced tumors showed upregulated expression of insulin receptor substrate 1 and phosphorylated forms of *IGF1* receptor and *Akt*, a finding consistent with the activation of *IGF* signaling [43]. This accumulating evidence would indicate that *FOXG1* expression and *PI3K* pathway activation may independently or in combination mediate resistance to *TGF-β*

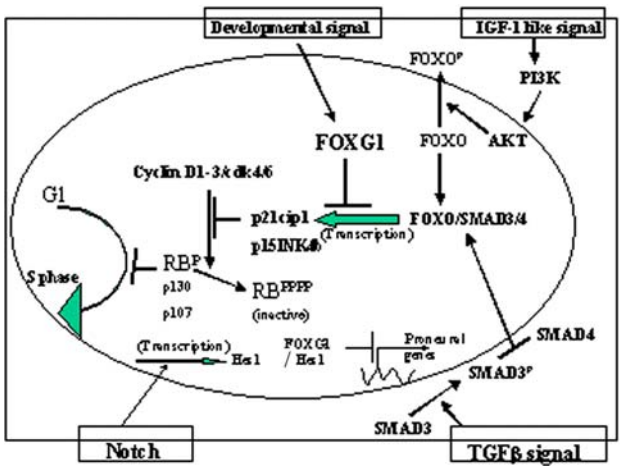


**Fig. 6** Pathway interaction for FOXG1: Schematic illustrating the reported role of *FOXG1* in inhibiting the transcriptional activity of *TGFβ* induced *FOXO/Smad3/4* complex, resulting in the down regulation of the transcription of *p21cip1* which among other functions inhibits G1 to S phase transit. *FOXG1* also forms a transcriptional repressor complex with *Hes1* (transcription upregulated by activated *Notch* signaling) resulting in the inhibition of the transcription of proneural genes thus suggesting that aberrant upregulation of *FOXG1* may partially account for persistence of an undifferentiated component in medulloblastomas

induced cytostasis. It is reasonable to speculate that combined *IGF* signaling induced phosphorylation of *FOXO* via *akt* and aberrant *FOXG1* upregulation may have additive effects in the opposition of *TGF-β* induced cytostasis in medulloblastoma cell lines and tumors.

Current studies implicate *Notch2*-mediated signaling in the growth of medulloblastoma [44]. In addition, *shh* signaling implicated in the growth of medulloblastoma has been demonstrated to mediate some of its biologic effects through the activation of N*otch2*-mediated signaling [45, 46]. It is also noteworthy that *FOXG1* has been implicated in the repression of neuronal differentiation by forming transcriptional repressor complexes with *Groucho/TLE* proteins, histone deacetylases and *Hes1* to effect the *Notch* activation-mediated negative regulation of proneural differentiation genes [47]. These observations suggest a major regulatory role for *FOXG1* at the critical points of transcriptional regulation by the *PI3K-akt*, *Notch, Shh via Notch2* and *TGF-β* signaling pathways.

We hypothesize that the role of *FOXG1* in medulloblastoma pathogenesis is (i) to maintain cerebellar neural stem-like cells in an undifferentiated state by forming transcriptional repressor complexes with effector proteins of the *Notch* signaling pathway such as *Hes1* that negatively regulate the expression of proneural genes, and (ii) to repress *TGF-β* induced cytostasis, thereby allowing the expansion of the progenitor population as occurs during neurogenesis [30]. These possible interactions between *FOXG1* and the *Notch* pathway in medulloblastoma are currently being explored to determine if they do occur in medulloblastomas as have been observed during neurogenesis. If such interactions are found in medulloblastoma, they will be consistent with a role for excess *FOXG1* expression secondary to gene copy gain/amplification in favoring progenitor cell overgrowth and providing the milieu for the accumulation of additional transforming genetic events and mutations. Thereafter, one may wonder if *FOXG1* fits the definition of a ''neoplasia susceptibility gene''. This determination awaits future studies.

**Acknowledgements** The supports of the Oklahoma Center for the Advancement of Science and Technology, the Moran Foundation and an equipment grant from the Presbyterian Health Foundation (AMA) are acknowledged.

## References

1. Giangaspero F, Bigner SH, Kleihues P, Pietsch T, Trojanowski JQ (2000) Medulloblastoma. In: Kleihues P, Cavenee WK (eds) Pathology & genetics: tumours of the nervous system. Publisher, IARC, Lyon
2. Raffel C, Jenkins RB, Frederick L et al (1997) Sporadic medulloblastomas contain PTCH mutations. Cancer Res 57:842–845
3. Zurawel RH, Chiappa SA, Allen C, Raffel C (1998) Sporadic medulloblastomas contain oncogenic β-catenin mutations. Cancer Res 58:896–899
4. Adesina AM, Dunn ST, Nalbantoglu J (2000) Expression of p27kip1 and p53 gene in medulloblastoma; relationship with cell proliferation and survival. Pathol Res Pract 196:243–250
5. Ray A, Ho M, Ma J et al (2004) A clinicobiological model predicting survival in medulloblastoma. Clin Cancer Res 10:7613–7620
6. Adesina AM, Nalbantoglu J, Cavenee WK (1994) p53 gene mutation and mdm2 gene amplification are uncommon in medulloblastoma. Cancer Res 54:5649–5651
7. Saylors RL 3rd, Sidransky D, Friedman HS et al (1991): Infrequent p53 gene mutations in medulloblastomas. Cancer Res 51:4721–4723
8. Gilbertson R, Wickramasinghe C, Hernan R et al (2001): Clinical and molecular stratification of disease risk in medulloblastoma. Br J Cancer 85:705–712
9. Bigner SH, Friedman HS, Vogelstein B, Oakes WJ, Bigner DD (1990) Amplification of the c-myc gene in human medulloblastoma cell lines and xenografts. Cancer Res 50:2347–2350
10. Aldosari N, Bigner SH, Burger PC et al (2002) MYCC and MYCN oncogene amplification in medulloblastoma. A fluorescence in situ hybridization study on paraffin sections from the Children's Oncology Group. Arch Pathol Lab Med 26:540–544
11. Brown HG, Kepner JL, Perlman EJ et al (2000) ''Large cell/anaplastic'' medulloblastomas: a Pediatric Oncology Group Study. J Neuropathol Exp Neurol 59:857–865
12. Herms J, Neidt I, Luscher B et al (2000) C-MYC expression in medulloblastoma and its prognostic value. Int J Cancer 89:395–402
13. Oliver TG, Grasfeder LL, Carroll AL et al (2003): Transcriptional profiling of the Sonic hedgehog response: a critical role for N-myc in proliferation of neuronal precursors. Proc Natl Acad Sci USA 100:7331–7336
14. Thompson MC, Fuller C, Hogg TL et al (2006): Genomics identifies medulloblastoma subgroups that are enriched for specific genetic alterations. J Clin Oncol 24:1924–1931
15. Tong C, Hui A, Yin XL et al (2004) Detection of oncogene amplifications in medulloblastomas by comparative genomic hybridization and array-based comparative genomic hybridization. J Neurosurg Spine 100:187–193
16. Ellison D (2002) Classifying the medulloblastoma: insights from morphology and molecular genetics. Neuropathol Appl Neurobiol 28:257–282
17. Hernan R, Fasheh R, Calabrese C et al (2003) ERBB2 up-regulates S100A4 and several other prometastatic genes in medulloblastoma. Cancer Res 63:140–148
18. Eberhart CG, Kratz J, Wang Y et al (2004) Histopathological and molecular prognostic markers in medulloblastoma: c-myc, N-myc, TrkC, and anaplasia. J Neuropathol Exp Neurol 63:441–449
19. Korshunov A, Savostikova M, Ozerov S (2002) Immunohistochemical markers for prognosis of average-risk pediatric medulloblastomas. The effect of apoptotic index, TrkC, and c-myc expression. J Neurooncol 58:271–279
20. Boon K, Eberhart CG, Riggins GJ (2005) Genomic Amplification of Orthodenticle Homologue 2 in Medulloblastomas. Cancer Res 65:703–707
21. Di C, Liao S, Adamson DC et al (2005) Identification of OTX2 as a medulloblastoma oncogene whose product can be targeted by all-trans retinoic acid. Cancer Res 65:919–924
22. Bale AE (1997) The nevoid basal carcinoma syndrome: Genetics and mechanisms of carcinogenesis. Cancer Invest 15:180–186
23. Hamilton SR, Liu B, Parsons RE et al (1995) The molecular basis of Turcot's syndrome. N Engl J Med 332:839–849

24. Levine AJ, Momand J, Finlay CA (1991) The p53 tumour suppressor gene. Nature 351:453–456
25. Arden K (2004) FoxO: linking new signaling pathways. Mol Cell 14:416–418
26. Yang YH, Dudoit S, Luu P, Peng V, Ngai J, Speed TP (2002): Normalization for cDNA microarray data: a robust composite method addressing single and multiple slide systematic variation. Nuclei Acid Res 30:e15
27. Draghici S (2003) Data pre-processing and normalization; In: Draghici S (eds) Data analysis tools for microarrays, Publisher, Chapman Hall/CRC, pp 309–340
28. Siegenthaler JA, Miller MW (2005): Transforming growth factor beta 1 promotes cell cycle exit through the cyclin-dependent kinase inhibitor p21 in the developing cerebral cortex. J Neurosci 25(38):8627–8636
29. Kasai M, Satoh K, Akiyama T (2005): Wnt signaling regulates the sequential onset of neurogenesis and gliogenesis via induction of BMPs. Genes Cells 10:777–783
30. Lu J, Wu Y, Sousa N, Almeida OF (2005) SMAD pathway mediation of BDNF and TGF beta 2 regulation of proliferation and differentiation of hippocampal granule neurons. Development 132:3231–3242
31. Ellison DW, Onilude OE, Lindsey JC et al (2005) United Kingdom Children's Cancer Study Group Brain Tumour Committee: beta-Catenin status predicts a favorable outcome in childhood medulloblastoma: the United Kingdom Children's Cancer Study Group Brain Tumour Committee. J Clin Oncol 23:7951–7957
32. Martynoga B, Morrison H, Price DJ, Mason JO (2005) *FOXG1* is required for specification of ventral telencephalon and region-specific regulation of dorsal telencephalic precursor proliferation and apoptosis. Dev Biol 283:113–127
33. Muzio L, Mallamaci A (2005) *FOXG1* Confines Cajal–Retzius Neuronogenesis and Hippocampal Morphogenesis to the Dorsomedial Pallium. J Neurosci 25:4435–4441
34. Hanachima C, Li SC, Shen L, Lai E, Fishell G (2004) *FOXG1* suppresses early cortical cell fate. Science 303:56–59
35. Dou C, Lee J, Liu B et al (2000) BF-1 Interferes with Transforming Growth Factor $\beta$ Signaling by Associating with Smad Partners. Mol Cell Biol 20:6201–6211
36. Seoane J, Le H-V, Shen L, Anderson SA, Massague J (2004): Integration of Smad and Forkhead Pathways in the Control of Neuroepithelial and Glioblastoma Cell Proliferation. Cell 117:211–223
37. Bourguignon C, Li J, Papalopulu N (1998) *XBF-1*, a winged helix transcription factor with dual activity has a role in positioning neurogenesis in Xenopus competent ectoderm. Development 125:4889–4900
38. Hanashima C, Shen L, Li SC, Lai E (2002) : Brain factor-1 controls the proliferation and differentiation of neocortical progenitor cells through independent mechanisms. J Neurosci 22:6526–6536
39. Xuan S, Baptista CA, Balas G, Tao W, Soares VC, Lai E (1995) Winged helix transcription factor BF-1 is essential for the development of the cerebral hemispheres. Neuron 14:1141–1152
40. Tao W, Lai E (1992): Telencephalon-restricted expression of BF-1, a new member of the HNF-3/fork head gene family in the developing rat brain. Neuron 8:957–966
41. Ahlgren S, Vogt P, Bronner-Fraser M (2003) Excess *FOXG1* Causes Overgrowth of the Neural Tube. J Neurobiol 57:337–349
42. Del Valle L, Enam S, Lassak A et al (2002) Insulin-like growth factor I receptor activity in human medulloblastomas. Clin Cancer Res 8:1822–1830
43. Rao G, Pedone CA, Del Valle L et al (2004) Sonic hedgehog and insulin-like growth factor signaling synergize to induce medulloblastoma formation from nestin-expressing neural progenitors in mice Oncogene 23:6156–6162
44. Fan X, Mikolaenko I, Elhassan I et al (2004) Notch1 and notch2 have opposite effects on embryonal brain tumor growth. Cancer Res 64:7787–7793
45. Hallahan AR, Pritchard JI, Hansen S et al (2004) The SmoA1 mouse model reveals that notch signaling is critical for the growth and survival of sonic hedgehog-induced medulloblastomas Cancer Res 64:7794–7800
46. Dakubo GD, Mazerolle CJ, Wallace VA (2006): Expression of Notch and Wnt pathway components and activation of Notch signaling in medulloblastomas from heterozygous patched mice. J Neurooncol 79:221–227
47. Yao J, Lai E, StifanI S (2001) The Winged-Helix Protein Brain Factor 1 Interacts with Groucho and Hes Proteins To Repress Transcription. Mol Cell Biol 21:1962–1972